

Contents lists available at [ScienceDirect](http://ScienceDirect)

## Scripta Materialia

journal homepage: [www.elsevier.com/locate/scriptamat](http://www.elsevier.com/locate/scriptamat)

## Regular Article

From glissile to sessile: Effect of temperature on  $\langle 110 \rangle$  dislocations in perovskite materials

Pierre Hirel\*, Philippe Carrez, Patrick Cordier

Unité Matériaux Et Transformations, Bât. C6, Univ. Lille 1, 59655 Villeneuve d'Ascq, France

## ARTICLE INFO

## Article history:

Received 14 January 2016

Received in revised form 16 March 2016

Accepted 1 April 2016

Available online 26 April 2016

## Keywords:

Perovskites

Dislocation

Climb

Fracture

Computer simulations

## ABSTRACT

In perovskite-type strontium titanate ( $\text{SrTiO}_3$ )  $\langle 110 \rangle$  dislocations, which are the main carriers of plastic flow at low temperature, lose their mobility as temperature increases, leading to brittle failure above 1050 K. We present theoretical evidence for a change in their core structure into a sessile, climb-dissociated configuration at high temperature. This mechanism is shown to operate in both  $\text{SrTiO}_3$  and  $\text{MgSiO}_3$ , indicating that it may be a general feature of perovskite-type materials. It follows that the activity of the  $\langle 110 \rangle$  slip system depends critically on the strain rate-temperature couple,  $(\dot{\epsilon}, T)$ .

© 2016 Elsevier Ltd. This is an open access article under the CC BY-NC-ND license (<http://creativecommons.org/licenses/by-nc-nd/4.0/>).

The discovery of the atypical mechanical behavior of strontium titanate ( $\text{SrTiO}_3$  or STO) and its double ductile-brittle-ductile transition [1,2] has challenged our understanding of the plastic behavior of perovskite-type materials, and has since motivated several studies. A series of experiments [3,4] and simulations [5,6] have provided a good understanding of the ductile behavior of STO at low temperature and demonstrated its direct link with the glide of  $\langle 110 \rangle$  dislocations. However it is still unclear why this mechanism becomes inactive at high temperature, leading to brittle failure above 1050 K. It was initially proposed that  $\langle 110 \rangle$  dislocations become sessile by dissociating into two  $\langle 100 \rangle$  dislocations, or because of a change of preferential slip plane [2]. Later it was proposed that  $\langle 110 \rangle$  dislocations dissociate by climb at high temperature, into a configuration similar to the one observed in low-angle tilt grain boundaries [7,3]. Despite arguments in favor of the latter [8], there has been no direct evidence for this change of core structure, the mechanisms by which it operates are still unknown, and whether this transition is specific to STO or a general feature of perovskite-type materials remains an open question.

In this work we investigate the effect of temperature on the core structure of individual  $[110]_{\text{pc}}$  edge dislocations in two perovskite-type materials: the cubic strontium titanate, and the orthorhombic, high-pressure magnesium silicate  $\text{MgSiO}_3$  which is the pure Mg end-member of bridgmanite [9], the main constituent of the Earth's lower mantle. In the following we consider  $\text{MgSiO}_3$  under the hydrostatic pressure of 30 GPa, corresponding to a depth of ca. 700 km i.e. the

uppermost lower mantle. Throughout this article crystal directions are given in the (pseudo-)cubic reference, noted with the subscript "pc", for easier comparison between the two materials (in  $\text{MgSiO}_3$   $[110]_{\text{pc}} = [100]$ ;  $[\bar{1}\bar{1}0]_{\text{pc}} = [010]$ ;  $2[001]_{\text{pc}} = [001]$ , see e.g. Ref. [10]). The  $\langle 110 \rangle_{\text{pc}}$  dislocations belong to the easiest slip system in both materials [11], [6]. Atomic systems were constructed with Atomsk [12], and classical molecular statics and dynamics simulations were performed with LAMMPS [13]. Interatomic interactions in  $\text{SrTiO}_3$  were modeled with the rigid-ion potential proposed by Thomas et al. [14], and in  $\text{MgSiO}_3$  with the one from Alfredsson et al. [15].

The glide-dissociated core structures of  $[110]_{\text{pc}}$  edge dislocations were modeled by structural optimization in both materials [11,6]. The size of atomic systems is about  $220 \text{ \AA} \times 130 \text{ \AA} \times c$ , verified to be large enough to ensure converged results. In STO the unit length  $c$  of dislocation line corresponds to one unit cell length  $[001]$ , i.e. the width of one layer of octahedra,  $c(\text{STO}) = 3.905 \text{ \AA}$ . Because  $\text{MgSiO}_3$  has a lower symmetry, the unit line length is  $2[001]_{\text{pc}}$ , i.e. the width of two layers of octahedra,  $c(\text{MgSiO}_3) = 6.709 \text{ \AA}$ . The ground-state dislocation configurations are represented in Fig. 1a and c. In STO these dislocations dissociate in their  $(\bar{1}\bar{1}0)$  glide plane into two collinear partials of Burgers vector  $b = 1/2[110]$  separated by an anti-phase boundary (APB) of extension  $d = 40 \text{ \AA}$  [11]. In high-pressure  $\text{MgSiO}_3$ ,  $[110]_{\text{pc}}$  edge dislocations also spread in their  $(\bar{1}\bar{1}0)_{\text{pc}}$  glide plane, but with a much more compact core of width  $d = 13 \text{ \AA}$ . This core structure remains identical in a wide range of pressures, from 30 to 140 GPa [6].

The high temperature core structures of the dislocations are obtained by performing molecular dynamics (MD) simulations for 10 to 20 ps at high temperature. A time step of 1 fs is used, and temperature is

\* Corresponding author.

E-mail address: [pierre.hirel@univ-lille1.fr](mailto:pierre.hirel@univ-lille1.fr) (P. Hirel).

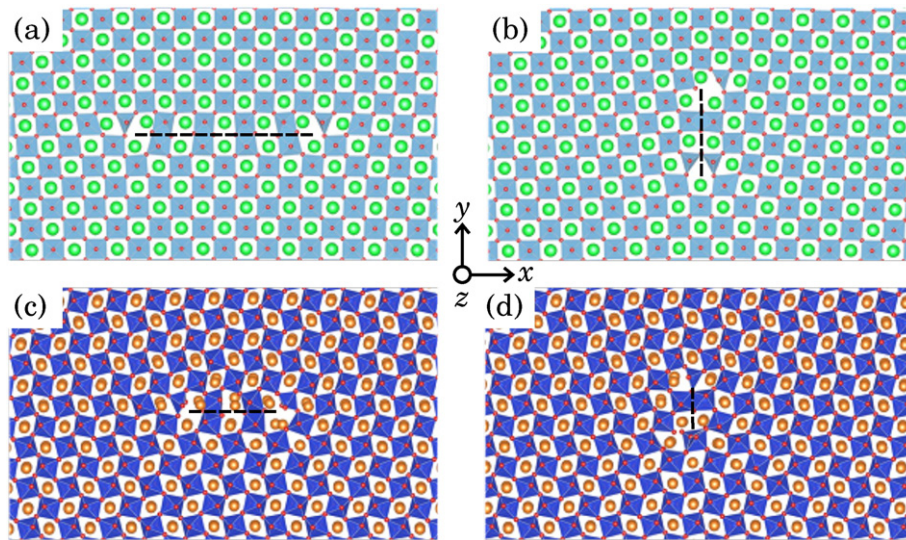


**Fig. 1.** The core structures of the  $[110]_{pc}$  edge dislocation in (a,b)  $\text{SrTiO}_3$ , (c,d)  $\text{MgSiO}_3$ . Sr or Mg ions are displayed as large spheres, Ti or Si ions as medium spheres, and oxygen as small red spheres;  $\text{O}_6$  octahedra are shown in transparent blue. The crystal directions are  $x = [110]_{pc}$ ,  $y = [1\bar{1}0]_{pc}$  and  $z = [001]_{pc}$ . The anti-phase boundaries (APB) in dislocation cores are overlaid by a dashed line. (a,c) At low temperature the dislocations are dissociated in their  $(1\bar{1}0)_{pc}$  glide plane. (b,d) At high temperature the dislocations dissociate in their  $[110]_{pc}$  climb plane.

maintained with a Nose-Hover thermostat. In order to accelerate thermally activated processes, very high temperatures are used (3000–4000 K), allowing to observe the change of core structure in times accessible to MD. During the simulations the dislocations either remained glide-dissociated, or produced a climb-dissociated configuration. Several MD simulations are performed to obtain a good sampling of climb-dissociated configurations. All simulations produced similar climb-dissociated dislocation cores, with the cations at the same positions, and they remained identical even after several 100 ps of MD at high temperature. The only noticeable differences between the different configurations obtained are the positions of oxygen ions, due to their high diffusivity in both materials. The configurations are optimized thanks to a conjugate-gradients algorithm, and the ones of lowest energy are represented in Fig. 1b and d. In STO the dislocation dissociates in its climb plane, with an APB spread in the  $(110)$  plane. The climb APB extends over a distance of 14.3 Å, separating two pairs of Sr ions. This core structure is indeed very similar to climb-dissociated dislocation arrays observed in low-angle grain boundaries [16,3], except that in the latter the distance between partial dislocations is imposed by the tilt angle. In  $\text{MgSiO}_3$ , the dislocation also dissociates in its  $(110)_{pc}$  climb plane (Fig. 1d), with an extension of about 7.37 Å, smaller than in STO. In both materials the climb-dissociated configuration is more stable than the glide-dissociated core, by 0.29 and 0.74 eV/Å in STO and  $\text{MgSiO}_3$ , respectively.

At low temperature the dislocations do not spontaneously switch to the lower-energy climb-dissociated core because this transformation requires the crossing of an energy barrier. We evaluate these barriers by means of the nudged elastic band (NEB) method [17]. The initial and final configurations are the glide- and climb-dissociated core structures, respectively, and NEB calculations employ from 8 to 32 images. The resulting minimum energy paths (MEP) are presented in Fig. 2. In STO, the first configurations along the MEP correspond to the decrease of the distance between the two partials. The inset of Fig. 2 shows an intermediate configuration that is similar to the one in  $\text{MgSiO}_3$  (Fig. 1c). Only when the dissociation distance becomes small enough does the dislocation switch to its climb-dissociated configuration. The total energy barrier is estimated to 3.44 eV/c, or 0.88 eV/Å. Thus, the effect of temperature is first to reduce the dissociation width, and then to induce the transformation to the climb-dissociated core structure.

In the case of  $\text{MgSiO}_3$ , due to the lower symmetry and the doubling of the unit length along the dislocation line ( $c = 2[001]_{pc}$ ), the reaction

path is more complex. Climb dissociation happens in successive steps, associated with three consecutive energy barriers (squares in Fig. 2). The first barrier corresponds to the change of core structure of the dislocation in the first half-plane of octahedra ( $0 \leq z < c/2$ ), yielding an activation energy about 0.013 eV/Å, significantly smaller than for STO. This is due to the fact that in STO the dislocation has to reduce its spreading in the glide plane before switching to a climb configuration, while in  $\text{MgSiO}_3$  the dislocation already has a compact core and can change its configuration more easily. Then, the dislocation changes its core structure in the second half-plane ( $c/2 \leq z < c$ ), with an energy barrier about 0.042 eV/Å. Finally, the third barrier with a height about 0.04 eV/Å corresponds to the rearrangement of oxygen ions inside the dislocation core, which further stabilizes the climb-dissociated configuration.

It is decisive that this transformation is hardly reversible. Once the core structure has changed it is very difficult to transform it back into the glide-dissociated configuration, because the activation energy is much larger. This can be related to yield stress anomalies in intermetallic compounds, triggered by dislocations adopting a sessile core structure at high temperature, eventually leading to locking and dislocation starvation [18].

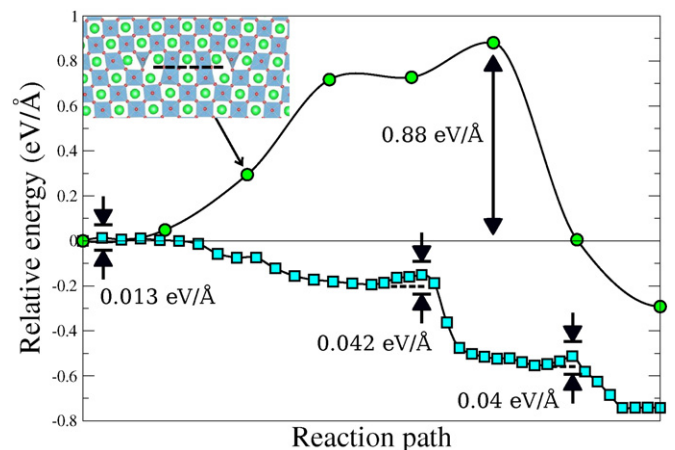


**Fig. 2.** Minimum energy paths for the transition from the glide-dissociated to the climb-dissociated configurations in  $\text{SrTiO}_3$  (circles) and  $\text{MgSiO}_3$  (squares). The glide-dissociated configurations serve as the reference of energy. The inset shows an intermediate configuration in STO where the dissociation distance is reduced compared to Fig. 1a.

The aforementioned activation energies correspond to the transformation of infinite, straight dislocation lines. In order to obtain a more realistic picture we compute the energy of formation of a climb-dissociated segment of width  $w$  along a long glide-dissociated dislocation of length  $L = 20c$ . The atomic configurations were constructed by concatenation of glide- and climb-dissociated segments. In STO the glide-dissociated segments have the configuration shown in the inset of Fig. 2, first to account for the reduced dissociation width at high temperature, and second to use a configuration similar to the one in MgSiO<sub>3</sub>. The climb-dissociated segments have the configuration shown in Fig. 1b. In MgSiO<sub>3</sub>, the glide and climb-dissociated segments are simply the ones shown in Fig. 1c and d. This situation is similar to the nucleation and propagation of kinks or jogs along a dislocation line. The formation of a climb-dissociated segment involves the formation of a pair of constriction jogs, each one having an energy  $U_j$ , and interacting with an energy  $U_{ij}$ . In addition, the climb-dissociated segment contributes with an energy  $U_c$  that is negative compared to the glide-dissociated segment. Then, the propagation of the jogs along the dislocation line reduces their interaction, and increases the energy gain  $U_c$ .

Fig. 3 shows the relative energy of the dislocation line as function of  $w$ . In STO the energy increases at first, reaching 15 eV for a dissociation width of  $2c$ . It means that the constriction jogs between glide- and climb-dissociated segments have a high energy cost. For greater widths the energy decreases linearly with a slope given by the contribution  $U_c$ , which is estimated to  $U_c = -0.58$  eV/Å. This energy is equal to the energy difference between the glide-dissociated configuration (inset of Fig. 2) and the climb-dissociated one. The energy of formation of the jogs can be determined by extrapolating the linear part of the curve (dashed line in Fig. 3), and is estimated to  $2U_j = 20.88$  eV.

By contrast, in MgSiO<sub>3</sub> the formation of a small climb-dissociated segment is sufficient to decrease the energy of the dislocation line. The energy of a climb-dissociated segment is estimated to  $U_c = -0.74$  eV/Å, i.e. very close to the value determined previously ( $-0.74$  eV/Å). The energy of a constriction jog is estimated to  $2U_j = 2.07$  eV, i.e. one order of magnitude smaller than in STO. Thus, it is much easier for climb-dissociated segments to form in MgSiO<sub>3</sub> than it is in STO.

In summary, in perovskite materials deformed at high temperature there is a competition between the applied stress  $\sigma$ , or strain rate  $\dot{\epsilon}$ , causing dislocations to glide with their glide-dissociated configuration, and temperature  $T$  that promotes the transformation of edge segments into their climb-dissociated configuration. At low temperature and high strain rate, dislocations glide easily and do not have time to change their

core structure. At high temperature and low strain rate, dislocations are almost immobile and their edge segments can transform into the climb-dissociated configuration. Between those two end-case scenarios, it can be expected that the activated mechanisms strongly depend on the  $(\dot{\epsilon}, T)$  couple, as schematically illustrated in Fig. 4.

In SrTiO<sub>3</sub> deformed at the strain rate  $\dot{\epsilon} = 10^{-4}$  s<sup>-1</sup>, like in the experiments in Ref. [1,2], increasing the temperature changes the balance between the possible mechanisms. At low temperature the  $\langle 110 \rangle$  dislocations are very mobile and allow for significant plastic flow. As the temperature increases, edge segments of the dislocations progressively transform into the climb-dissociated configuration and act as pinning points, leading to strain hardening at first. When temperature is high enough more and more dislocation segments become sessile, eventually leading to brittle failure around 1050 K. In SrTiO<sub>3</sub> deformed at high temperature, long, straight dislocations of pure edge character were observed [3]. These dislocations do not appear to be dissociated in their glide plane, indicating that they may be in their climb-dissociated configuration. Considering the aforementioned energy path, it can be expected that slower strain rates would grant dislocations more time to change their core structure, thus causing the ductile-brittle transition to shift towards lower temperatures. On the contrary, using higher strain rates would shift it towards higher temperatures.

The same arguments apply to the deformation of MgSiO<sub>3</sub>. When deformed at  $T = 1200$  K and strain rates typical to the laboratory, one observes the glide of  $\langle 110 \rangle_{pc}$  dislocations [10]. However in the conditions of deformation of the Earth's lower mantle ( $T = 1500 - 4000$  K,  $\dot{\epsilon} = 10^{-12}$  to  $10^{-16}$  s<sup>-1</sup>), dislocations have an extremely low mobility and a lot of time to transform into their climb-dissociated core structure. As a result glide is completely inhibited. As illustrated in Fig. 4, at a given temperature  $T$ , the mechanisms that are activated in laboratory conditions, i.e. dislocation glide under  $\dot{\epsilon} = 10^{-4}$  s<sup>-1</sup>, cannot be extrapolated to the strain rates of the lower mantle. In the latter  $\langle 110 \rangle_{pc}$  dislocations are sessile, i.e. they cannot move by glide anymore. The high temperature creep conditions may allow them to move by pure climb mechanisms by absorbing or emitting vacancies. Similarly, if SrTiO<sub>3</sub> were deformed at very slow strain rates, it is possible that it may also deform by pure climb mechanisms instead of going through brittle failure.

As previously pointed out, the change of core structure is easier in MgSiO<sub>3</sub> than in SrTiO<sub>3</sub>. Indeed in the former the dislocation is compact and easily dissociates by climb, with a small activation energy. In the latter the wide initial spreading makes climb dissociation less immediate. It is necessary to reduce the distance between the two partial dislocations

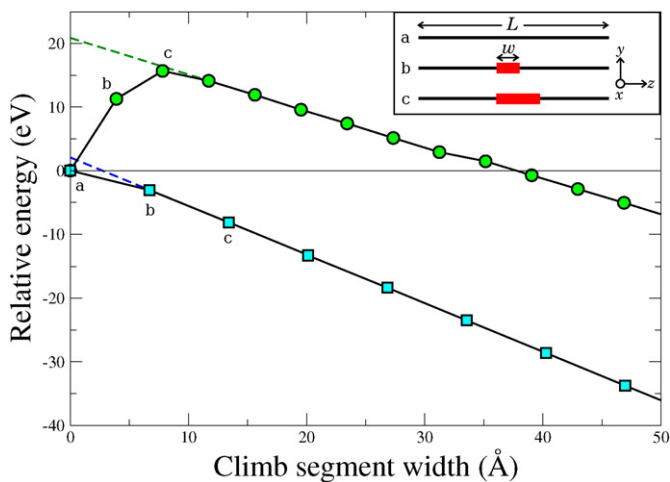


Fig. 3. Relative energy of the dislocation line for various widths  $w$  of climb-dissociated segments in SrTiO<sub>3</sub> (circles) and MgSiO<sub>3</sub> (squares). Letters correspond to the illustrations in the inset: (a) Initial glide-dissociated dislocation of length  $L$ . (b) Formation of a climb-dissociated segment of width  $w$ , displayed as a thick line. (c) Propagation of the climb-dissociated segment. The Cartesian directions  $x, y, z$  are the same as in Fig. 1.

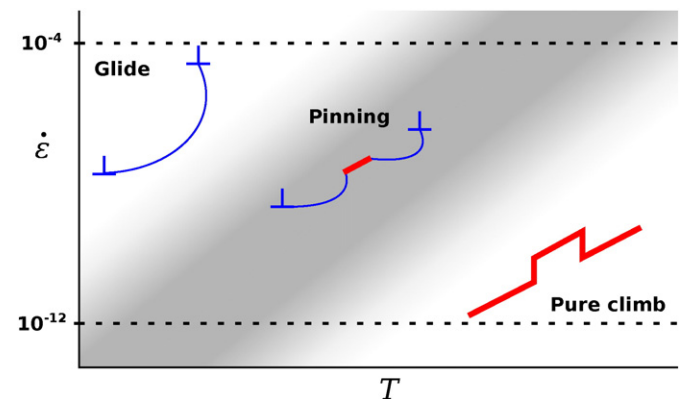


Fig. 4. Schematic illustration of the expected behavior of  $\langle 110 \rangle_{pc}$  dislocations in perovskite materials, as a function of temperature  $T$  and strain rate  $\dot{\epsilon}$ . Thin blue lines represent the dislocation in its glide-dissociated configuration, and thick red lines the sessile climb-dissociated configuration. Horizontal dashed lines indicate the strain rates typical of the laboratory ( $\dot{\epsilon} \approx 10^{-4}$  s<sup>-1</sup>) and to the Earth's lower mantle ( $\dot{\epsilon} \leq 10^{-12}$  s<sup>-1</sup>). The actual ranges of activation for each mechanism depend on the chemical composition of the perovskite.

before climb dissociation can occur, and this has a large energy cost of its own. In potassium niobate ( $\text{KNbO}_3$ ), another perovskite-type material, it was recently observed that  $\langle 110 \rangle$  edge dislocations have a dissociation distance  $d = 60 \text{ \AA}$  [19], even wider than in  $\text{SrTiO}_3$ . Thus, it can be expected that the energy required to reduce the distance between the two partials and allow climb dissociation is even larger. Experimental observations show that  $\langle 110 \rangle$  dislocations are still observed in  $\text{KNbO}_3$  deformed at high temperature [20], [19], indicating that they are still glissile and have not dissociated by climb. These observations support the hypothesis that the initial spreading of the dislocation is directly correlated with the difficulty to dissociate by climb. In perovskite materials where  $\langle 110 \rangle$  dislocations are very widely dissociated, it is possible that climb dissociation never occurs even at very high temperature. In summary, climb dissociation may be triggered easily in some perovskites, and with more difficulty or not at all in others, depending on the chemical composition and spreading of  $\langle 110 \rangle_{\text{pc}}$  dislocations.

It is important to note that the present results correspond to the change of core structure as a conservative process (i.e. at constant number of atoms). At high temperature point defects may interact with dislocations and alter the reaction path for climb dissociation. For instance, recent simulations have shown that the absorption of a Si vacancy is sufficient to induce the climb dissociation of an edge dislocation in  $\text{MgSiO}_3$ , even without the help of temperature [19]. The effect of point defects on climb dissociation, and on subsequent motion by climb, need to be addressed separately.

Finally, in conditions where the easiest  $\langle 110 \rangle_{\text{pc}}$  slip system is inhibited, other deformation mechanisms may be activated, like point defects diffusion, grain boundary sliding, or other slip systems. For instance the  $\langle 100 \rangle$  slip system becomes active in  $\text{SrTiO}_3$  deformed above 1270 K [3], allowing for a new ductile regime. There are also indications of  $\langle 100 \rangle_{\text{pc}}$  slip in  $\text{KNbO}_3$  deformed above 800 K [20,19], and in  $\text{MgSiO}_3$  deformed at 26 GPa and 2023 K [21]. The  $\langle 100 \rangle_{\text{pc}}$  dislocations have a compact core and cannot dissociate by climb, so this slip system becomes the easiest

one when  $\langle 110 \rangle_{\text{pc}}$  slip is not possible. Their role in the high temperature creep of perovskites remains to be determined.

## Acknowledgements

This work was supported by funding from the European Research Council under the Seventh Framework Programme (FP7), ERC grant N.290424—RheoMan.

## References

- [1] D. Brunner, S. Taeri Baghadrani, W. Sigle, M. Rühle, *J. Am. Ceram. Soc.* 84 (2001) 1161–1163.
- [2] P. Gumbsch, S. Taeri Baghadrani, D. Brunner, W. Sigle, M. Rühle, *Phys. Rev. Lett.* 87 (2001) 085505.
- [3] W. Sigle, C. Sarbu, D. Brunner, M. Rühle, *Philos. Mag.* 86 (2006) 4809–4821.
- [4] M. Castillo Rodríguez, W. Sigle, *Scr. Mater.* 64 (2011) 241–244.
- [5] P. Carrez, D. Ferré, C. Denoual, P. Cordier, *Scr. Mater.* 63 (2010) 434–437.
- [6] P. Hirel, A. Krach, P. Carrez, P. Cordier, *Acta Mater.* 79 (2014) 117–125.
- [7] T. Mitchell, A. Heuer, *Dislocations in Solids*, Vol. 12 Elsevier Science Bv, Amsterdam, 2004 339–402.
- [8] T. Mitchell, *Ceramics Science and Technology*, Vol.2: Materials and Properties, vol. 2, Wiley-VCH Verlag GmbH & Co. KGaA, 2010 379–436.
- [9] O. Tschauner, C. Ma, J. Beckett, C. Preschner, V. Prakapenka, G. Rossman, *Science* 346 (2014) 1100–1102.
- [10] P. Cordier, T. Ungár, L. Zsoldos, G. Tichy, *Nature* 428 (2004) 837–840.
- [11] P. Hirel, M. Mrovec, C. Elsässer, *Acta Mater.* 60 (2012) 329–338.
- [12] P. Hirel, *Comput. Phys. Commun.* 197 (2015) 212–219.
- [13] S. Plimpton, *J. Comp. Physiol.* 117 (1995) 1–19 (URL: <http://lammps.sandia.gov>).
- [14] B. Thomas, N. Marks, B.D.Begg, *Nucl. Inst. Methods Phys. Res. B* 228 (2005) 288–292.
- [15] M. Alfreðsson, J. Brodholt, D. Dobson, A. Oganov, C. Catlow, S. Parker, G. Price, *Phys. Chem. Miner.* 31 (2005) 671–682.
- [16] R. De Souza, J. Fleig, J. Maier, O. Kienzle, Z. Zhand, W. Sigle, M. Rühle, *J. Am. Ceram. Soc.* 86 (2003) 922–928.
- [17] G. Henkelman, H. Jónsson, *J. Chem. Phys.* 113 (2000) 9978.
- [18] P. Veyssi re, *Mater. Sci. Eng. A* 309–310 (2001) 44–48.
- [19] P. Hirel, P. Carrez, E. Clouet, P. Cordier, *Acta Mater.* 106 (2016) 313–321.
- [20] S. Beauchesne, J. Poirier, *Phys. Earth Planet. Inter.* 61 (1990) 182–198.
- [21] N. Miyajima, T. Yagi, M. Ichihara, *Phys. Earth Planet. Inter.* 174 (2009) 153–158.